coatings

MDPI

Article

Investigating the Synergistic Effect of Electrochemical Texturing and MoSeC Coatings on the Frictional Behaviour of Lubricated Contacts

Manoj Rajankunte Mahadeshwara [1], Fátima Rosa [1], Todor Vuchkov [1,2], Luís Vilhena [1], Amílcar Ramalho [1], Pooja Sharma [1] and Albano Cavaleiro [1,2,*]

[1] CEMMPRE Mechanical Engineering Department, University of Coimbra, 3030-788 Coimbra, Portugal
[2] IPN—LED & MAT, Instituto Pedro Nunes, Rua Pedro Nunes, 3030-199 Coimbra, Portugal
* Correspondence: albano.cavaleiro@dem.uc.pt

Abstract: The materials used for the piston cylinders of automobile engines, or the ring and tappets of various mechanical components, are continuously experiencing lubricated sliding motions. These surfaces are prone to damage due to the various tribological aspects of friction and wear. Hence, enhancing their surface properties would contribute to increasing their life and saving energy and resources. For many decades surface texturing and surface coating technology have been studied to improve the surface tribological behaviours of the materials. In the present study, the steel surface was textured with electrochemical processing (ECP) and post-coating with transition metal dichalcogenides (TMD) using a molybdenum-selenium-carbon (MoSeC) film. A comparative study was conducted to investigate the synergistic effect of surface texturing and coating to improve frictional properties on the steel surface. The block-on-ring experiments were performed under lubricated conditions to understand the improvement of COF at different lubrication regimes. It has been seen that the MoSeC-coated circular patterns exhibited improvements in the frictional properties at all the lubricated conditions if compared with smooth surfaces.

Keywords: ECP texturing; MoSeC coating; lubrication regimes

Citation: Mahadeshwara, M.R.; Rosa, F.; Vuchkov, T.; Vilhena, L.; Ramalho, A.; Sharma, P.; Cavaleiro, A. Investigating the Synergistic Effect of Electrochemical Texturing and MoSeC Coatings on the Frictional Behaviour of Lubricated Contacts. *Coatings* **2023**, *13*, 692. https://doi.org/10.3390/coatings13040692

Academic Editors: Mohamed El Garah and Frederic Sanchette

Received: 8 March 2023
Revised: 22 March 2023
Accepted: 23 March 2023
Published: 28 March 2023

1. Introduction

Friction reduction in mechanical components is necessary to improve the tribological properties that help in saving energy and resources. Many research groups across the world have worked on friction reduction, thereby enhancing the tribological properties of the materials by improving their surface properties [1–5]. Surface texturing is one of the surface engineering techniques that play an important role in improving surface tribological properties by enhancing the load-bearing capacity of the material under lubricated contact conditions [6]. Producing the micro-dimple patterns on the material surface tends to create hydrodynamic pressure at these dimples. This helps in the formation of thick lubricant films on the surface between the solid–solid contact resulting in friction reduction at the material interface [7–9]. There are different texturing techniques, such as laser surface texturing (LST), micro-electro discharge machining (EDM), abrasive water jet machining, and ion beam machining, among others. However, these techniques have their own limitations, such as mechanical and thermal damage on the surface of the materials [10,11]. Additionally, some of these techniques form burrs and debris on the textured surface, which could be solved using the ECP technique. The big advantage of this is that in the case of ECP, the debris and the burrs which are formed are dissolved electrochemically [12]. The texturing process with ECP was conducted through the anodic dissolution of the workpiece through electrolysis. The material in the workpiece was removed atom by atom hence replicating the desired pattern of the electrode [13]. Different researchers have studied the improvements in tribological properties by implementing the texturing using the ECP

method [14–16]. The friction reduction using the ECP technique was studied by Jung won et al. [14]. They investigated AISI 440C steel specimens textured by the micro-ECP method and observed a reduction in friction for the textured specimens compared to the smooth specimen. Furthermore, studies on surface improvements were conducted, where the surface and mechanical properties of the 304 stainless steel were improved by the combination of two processes, micro-EDM and ECM, which also increased the efficiency of the machine [15]. Chen et al. achieved a reduction in COF on micro dimple (ECP), textured, and chrome-coated surfaces [16]. These studies confirm the important role of ECP texturing in improving the tribological properties of the materials.

Surface coatings play an important role in improving the tribological performance of materials, such as COF and wear rate. The importance of coatings in tribological contacts is well documented in the literature and identified the role of coating in providing easy shear mechanisms, hence solving the problems of liquid lubrication [17–19]. There are various types of solid lubricant coatings, such as diamond-like carbon (DLCs), TMD, tungsten carbide with carbon (WC/C) coatings, etc. Amongst these coatings, TMD coatings play a vital role in contributing better frictional properties on the material surface [20]. TMD coatings have the general formula X-M-X, where X stands for chalcogenides and M stands for transition metal atom. Weak van Der Waals bonds help provide beneficiary tribological properties, such as easy shear layers on the surface contact interface [21]. There are various types of metallic members in TMD coatings, such as WS_2, MoS_2, $MoSe_2$, etc., whose properties have been studied and identified by various researchers for their contribution to enhancing surface tribological behaviours [22–24]. The $MoSe_2$ has better oxidation resistance, and combining this metal with the chalcogenides such as carbon (C) improves the density, tribological, and mechanical properties of TMD coatings [25]. In a recent study, T.B. Yaqui et al. investigated the properties of MoSeC solid lubricant coatings showing the lowest COF of 0.025; hence, it showed the highest frictional stability in both humid air and dry nitrogen environments [17]. A comparative study was conducted by T. Poovar et al. on the tribological behaviour of the self-lubricating properties of WSC and MoSeC sputtered coatings. It was noted that WSC films were more thermally stable, and MoSeC had the lowest COFs in humid atmospheres [26]. Based on this reference, it was identified that the MoSeC TMD coatings improved the material surface's tribological properties, which helped in various applications.

In the present study, an investigation of the surface tribological properties of steel were performed using two surface modification techniques, i.e., texturing and coating. The surfaces were textured with a circular dimple geometric pattern using the ECP technique and were then post-coated with MoSeC and TMD films. The performance of these two techniques was investigated to understand their contribution to improving frictional properties. The comparative studies based on textured/non-textured surfaces and coated/non-coated surfaces were performed to understand their individual roles.

2. Materials and Methods

2.1. Specimens Preparation: Texturing & Coating

The molybdenum-based high-speed AISI M2 steel specimens (Natrater, Marinha Grande, Portugal) with a diameter of 24 mm and thickness of 7.9 mm were prepared for texturing. The chemical composition of the steels specimen as well as the counter body used during the tribological tests is shown in Table 1.

Table 1. Chemical composition of the specimens to be textured and coated and respective counter body (in weight %).

	Elements	C	Cr	Mn	Mo	Ni	V	Si	W
Specimen	AISI M2	1.00	4.15	0.30	5.00	-	1.95	0.30	6.25
Counter Body	AISI 3415	0.17	0.75	0.55	-	3.25	-	<0.20	-

The specimens were polished using SiC abrasive papers from 500 to 2000 Grit and diamond suspension of ~6 µm until a surface roughness R_a lower than ~0.04 µm was obtained and was ultrasonically cleaned with ethanol and acetone (duration 15 min). After cleaning, the specimens were textured using the ECP technique (PMM–Moldes, Maceira, Portugal) with circular (C) geometric patterns. The textured specimens prepared with this ECP technique are named ECP_S_C. The surface characterization of the specimen was performed using the interferometer by R-tech instruments, and their texture dimensions were obtained, as shown in Figure 1. Diameter (D) ~262 µm, Dimple depth (D_d) ~19 µm, and the distance between two dimples (D_s) ~306 µm. These dimensions are summarized in Table 2.

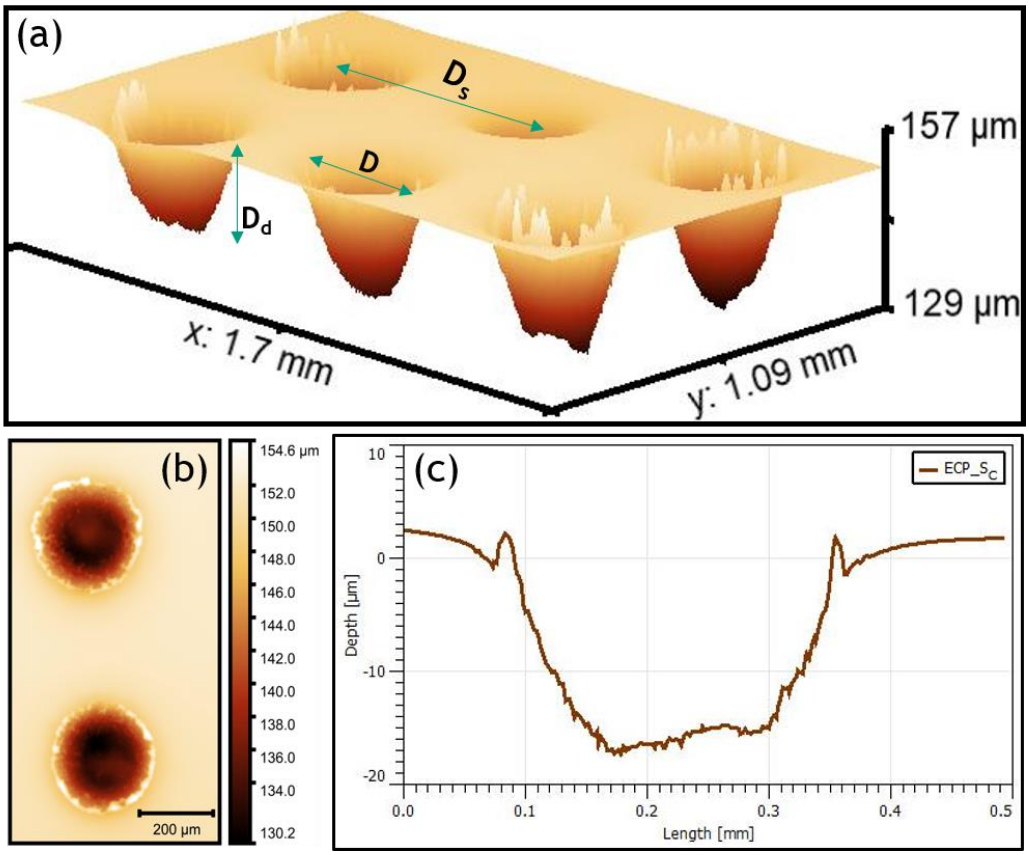

Figure 1. Surface profiles of the ECP textured specimens (ECP_S_C): (**a**) 3D surface image; (**b**) 2D image; (**c**) Surface profile of one dimple.

Table 2. Dimensions of textured specimens with circular patterns.

Specimens	D (µm)	D_d (µm)	D_s (µm)
ECP_S_C	262.7 ± 3.5	19.4 ± 1.4	306.6 ± 3.2

Further, the textured specimens were cleaned to undergo coating deposition. The TMD coating was performed using a closed-field unbalanced magnetron sputtering in a semi-industrial unit (Teer Coatings Ltd., Droitwich, Worcestershire, UK) using MoSeC as the coating material, as shown in Figure 2.

The deposition was performed in a vacuum chamber mounted with four targets (340 × 140 × 8 mm) consisting of two graphite, one $MoSe_2$ target, and one Cr target for the interlayer. The targets and textured specimens were first sputter cleaned in an Argon (Ar) gas atmospheric medium at a pressure of ~0.5 Pa, then the deposition of the elements was performed. The DC power supply (Advanced Energy's Pinnacle, Denver, CO, USA)

operated in the power control mode and was supplied to the targets and the substrates. The MoSeC film thickness of ~1.8 µm and hardness of ~4.3 GPa was obtained on the specimens. The hardness measurements were performed in a depth sensing indentation equipment (NanoTest platform, Micromaterials, Wrexham, UK). For film thickness measurements and a commercial profilometer was used (Mitutoyo Surftest SJ 500P profilometer, Elland, UK). The coated specimens were placed on a profilometer platform so that the diamond tip travelled across the surface of the sample during its movement. Since a mask was used to prevent the entire sample from being coated, it is thus possible to determine a difference in height between the coated and uncoated parts (film thickness) [17]. The coating parameters are summarised in Table 3.

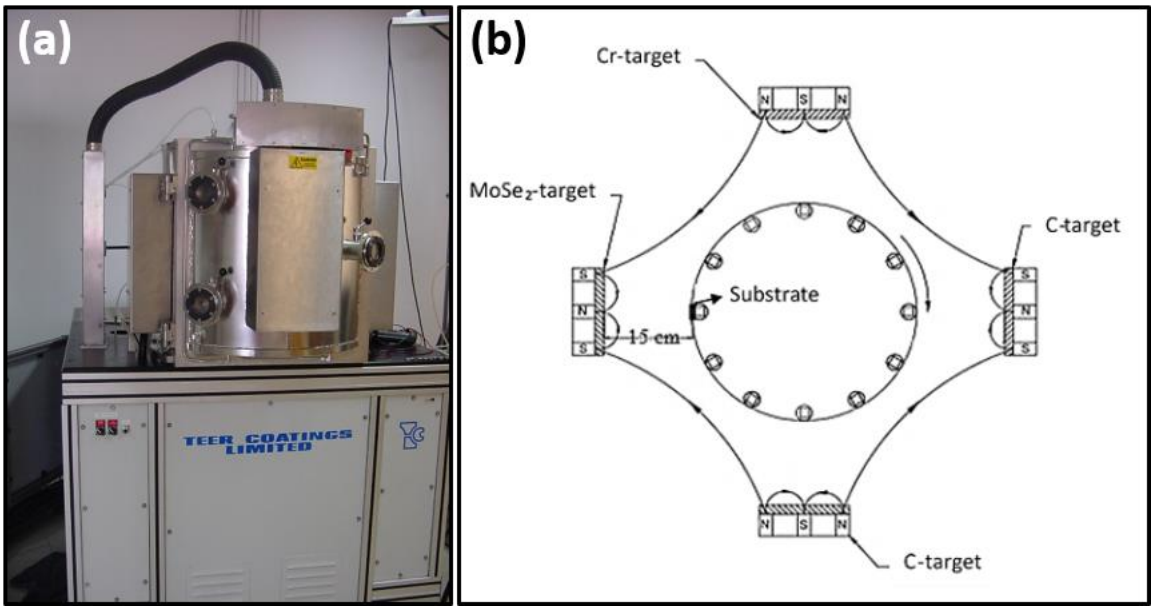

Figure 2. Closed-field unbalanced magnetron sputtering equipment: (**a**) External view; (**b**) Schematic picture from the targets inside the chamber.

Table 3. Coating parameters used for MoSeC coating.

Coating	Elemental Composition (At. %)					Thickness (µm)	Deposition Time (min)	Deposition Rate (nm/min)	Hardness (GPa)
	C	Se	O	Mo	Cr				
MoSeC	58.0	26.9	0.9	12.5	0.2	1.8	120	13.8	4.3

The characterization of the texture geometry of the tested and non-tested specimens was performed using the interferometer, scanning electron microscope (FESEM-Zeiss Merlin, Germany) with electron dispersive spectroscopy (EDS) to understand the reason behind the improvement in the tribological properties.

The specimens are named as S0 = smooth; S0_MoSeC = smooth + coated; ECP_Sc = circular dimple textured; ECP_Sc_MoSeC = circular dimple textured + MoSeC coated.

2.2. Tribology Testing

The coefficient of friction (COF) for the prepared specimens was determined using a block-on-ring configuration in an in-house tribometer, as shown in Figure 3. The working principle of this tribometer has already been described in previous works [27].

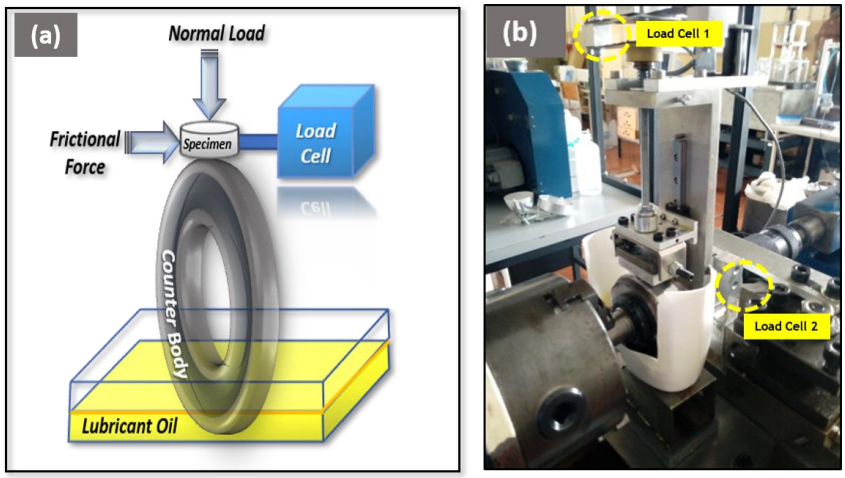

Figure 3. Tribometer used during experiments: (**a**) Schematic diagram of the block-on-ring configuration; (**b**) Tribometer showing the two load cells (1—load cell to measure normal force, 2—load cell to measure tangential force) and the contact conditions.

The rotating ring used in this setup was AISI 3145 steel with a diameter and width of 150 mm and 12 mm, respectively. The chemical composition of AISI 3145 steel is given in Table 1. The test was performed in fully flooded, lubricated conditions maintaining the specimen stationary against the rotating ring by applying a constant load of 25 N. The ring was submerged in the lubricated oil with a viscosity of 99 mPa.s at room temperature at 24 °C. The COF was measured using the attached load cells at nine different sliding speeds ranging between 0.01 m/s and 0.47 m/s. One specimen was used for each case. However, the COF value is an average of all the values acquired over the duration of the sliding test. For each specimen and for the entire sliding speed range, the calculated COF was plotted as a function of the Hersey number [28]. The understanding of the lubrication regimes was also conducted by calculating the Tallian parameter (λ), that is, the minimum film thickness at the contact interface between the specimen and the ring divided by the composite surface roughness [29]. The calculated values of the Hersey number (HN) and Tallian parameter (λ) are summarized in Table 4. In the identification of the lubricating regimes, it was considered that for $\lambda < 1$, the lubrication regime was Boundary, for $1 < \lambda < 3$ mixed, and for $\lambda > 3$ hydrodynamic.

Table 4. Hersey number (HN), Tallian parameter (λ), and different lubrication regimes as a function of the sliding speed (m/s).

Speed (m/s)	HN	(λ)	Lubrication Regimes
0.01	2.24×10^{-5}	0.7	Boundary Lubrication (BL)
0.02	1.49×10^{-5}	1.1	Mixed Lubrication (ML)
0.03	1.12×10^{-5}	1.4	
0.04	7.46×10^{-6}	1.7	
0.07	3.73×10^{-6}	2.5	
0.12	1.87×10^{-6}	4.4	Hydrodynamic Lubrication (HL)
0.23	1.31×10^{-6}	5.7	
0.31	9.33×10^{-7}	7.0	
0.47	5.60×10^{-7}	9.2	

The greatest limitation of the block on the ring configuration test produced the small contact width. For a further block on the ring, a reciprocating sliding test was conducted to ensure a greater number of dimples on the contact, in which a 100Cr6 ring (R_a lower than ~0.04 μm) with 8 mm inner diameter and 11 mm outer diameter was used, sliding against the S0 and ECP_S_C_MoSeC specimens. The applied force was 30 N, the stroke was

2 mm, and the average linear sliding speed varied between 2.7 and 22.3 mm/s. The test parameters are summarized in Table 5.

Table 5. Test conditions used in the reciprocating sliding test (lubricated with PAO 8—Polyalphaolefin 8, ν40 = 46 mm^2/s).

Test	Load (N)	Frequency (Hz)	Sliding Distance (mm)	Sliding Speed ($\times 10^{-3}$ m/s)	Sliding Time (s)
1	30	0.67	2000	2.7	746
2	30	1.25	2000	5.0	400
3	30	1.82	2000	7.3	275
4	30	3.40	2000	13.6	147
5	30	4.12	2000	16.5	121
6	30	5.57	2000	22.3	90

3. Results and Discussion

3.1. Friction Behaviour for Smooth and Smooth and Coated Specimens (S0 vs. S0_MoSeC)

Surface coating techniques are known to modify the surface properties of the materials, thereby improving their tribological behaviours. In this study, the coating was performed using TMD coating with MoSeC films, and their effects on the surface properties of the steel specimens were tested. To understand their effects on tribological properties, the smooth and coated specimen (S0_MoSeC) was compared with the smooth steel specimen (S0). The Stribeck curves were plotted for these specimens using the COF data obtained from the block-on-ring tests along with the calculated values of Hersey numbers.

The Stribeck curves are shown in Figure 4. The graphs show the performance of the smooth, coated, and just smooth steel specimens in different lubrication regimes. There was an improvement in frictional properties, as seen for the MoSeC coated specimen at BL and HL regimes in comparison to the smooth specimen. The contribution of surface coating reduced the friction at the solid–solid contacts, which occurred at the BL regime and to worked as a solid lubricant. By contrast, the decrease in friction for the MoSeC films was evident at the HL regime between 2.3% and 5.2%. According to previous studies, these properties of the TMD coatings were found only in the case of the MoSeC films due to their better tribological properties [30]. Most likely, during the mixed lubrication regime, the sliding speed was not yet high enough for the film to have hydrodynamic effects with lower friction. Additionally, at the same time, contact between surfaces was not close enough for the coating to function as a solid lubricant.

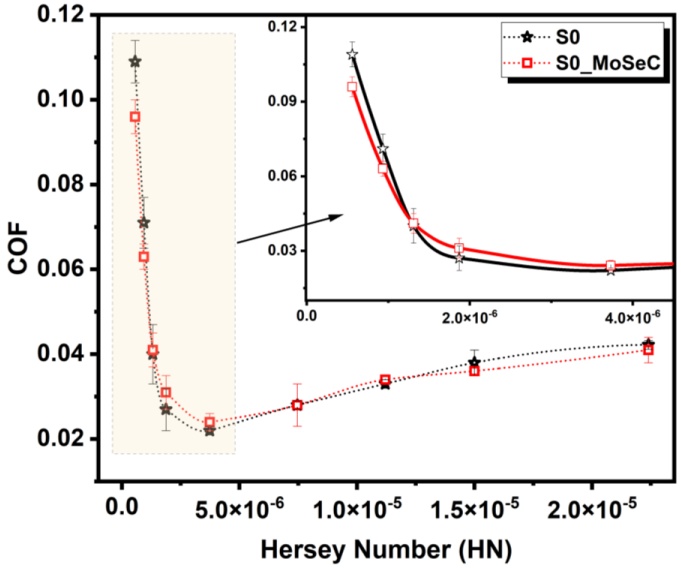

Figure 4. Stribeck curves for the S0 and S0_MoSeC specimens.

Thus, the contribution of the TMD surface coating for improving the frictional properties was observed at two lubrication regimes which proved the efficiency of these coatings for fully lubricated applications. The percentage improvement of the S0_MoSeC specimen with respect to the S0 specimen is tabulated in Table 6.

Table 6. Performance of the S0 and S0_MoSeC specimens (positive values are decreases in friction related to the smooth and uncoated specimen while negative values mean increases in friction).

Speed (m/s)	0.01	0.02	0.03	0.04	0.07	0.16	0.23	0.31	0.47
S0_MoSeC	11.9%	10.7%	−2.5%	−14.8%	−9.1%	−1.2%	−1.5%	5.2%	2.3%
S0	–	–	–	–	–	–	–	–	–

3.2. Friction Behaviour for the Smooth vs. ECP Textured Specimens

The effect of texturing the specimen can be analysed by making comparative studies of Stribeck curves for the smooth and textured specimen. Figure 5 shows the Stribeck curves for the smooth S0 and ECP textured; ECP_S_C specimen. From the Stribeck curves, it was observed that the circular textured specimen ECP_S_C performed with lower friction than the smooth specimen S0 during most parts of the sliding speed range (between 0.01 to 0.4 m/s).

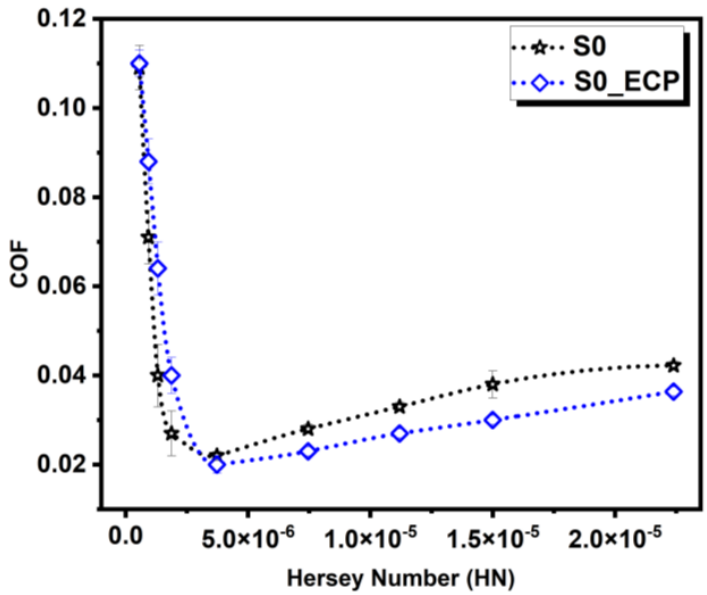

Figure 5. Stribeck curves of the specimens S0 and ECP_S_C.

The percentage improvements of the specimen ECP_S_C in comparison to the S0 smooth specimen are tabulated in Table 7.

Table 7. Performance of the S0 and ECP_S_C specimens (positive values are decreases in friction related to the smooth and uncoated specimen while negative values mean increases in friction).

Speed (m/s)	0.01	0.02	0.03	0.04	0.07	0.16	0.23	0.31	0.47
ECP_S_C	−0.9%	−23.9%	−60.0%	−48.1%	9.1%	17.8%	18.2%	21.0%	14.3%
S0	-	-	-	-	-	-	-	-	-

For the textured specimen, an improvement in the frictional properties in relation to the smooth surface (S0) was seen mainly at the HL regime. For the ECP_S_C specimen and rotational speeds from 0.07 m/s to 0.47 m/s, an improvement between 9% and 21% was observed. As can be seen, the ECP_S_C specimen contributed to the friction reduction in the HL regime, which proved that circular geometric patterns were best suited for

lubricated sliding contact applications in a wider range of contact conditions. The texture patterns retained the lubricants during the sliding motion and generated hydrodynamic pressure with a lift-up effect, thereby providing improved lubrication. Furthermore, the effect of the combination of both surface texturing and coatings was studied to understand their synergistic behaviours in improving the tribological properties of the textured and coated specimens.

3.3. Synergistic Effect of Coating and Texturing

3.3.1. Block on Ring

The synergistic effect of the texturing plus coating was studied due to its contribution to improving the frictional properties of the steel specimens at two different lubrication regimes (BL and HL). The tribological behaviour of the circular textured and circular-coated specimens was compared with the smooth and only coated specimen to understand their overall ability. This overall improvement in the tribological behaviour of ECP_S_C and ECP_S_C_MoSeC specimens confirmed the synergy of surface modification techniques via texturing and coating. Figure 6 shows the Stribeck curves for the specimens S0, S0_MoSeC, ECP_S_C, and ECP_S_C_MoSeC, and the percentage improvement in the friction level of all these specimens are summarized in Table 8.

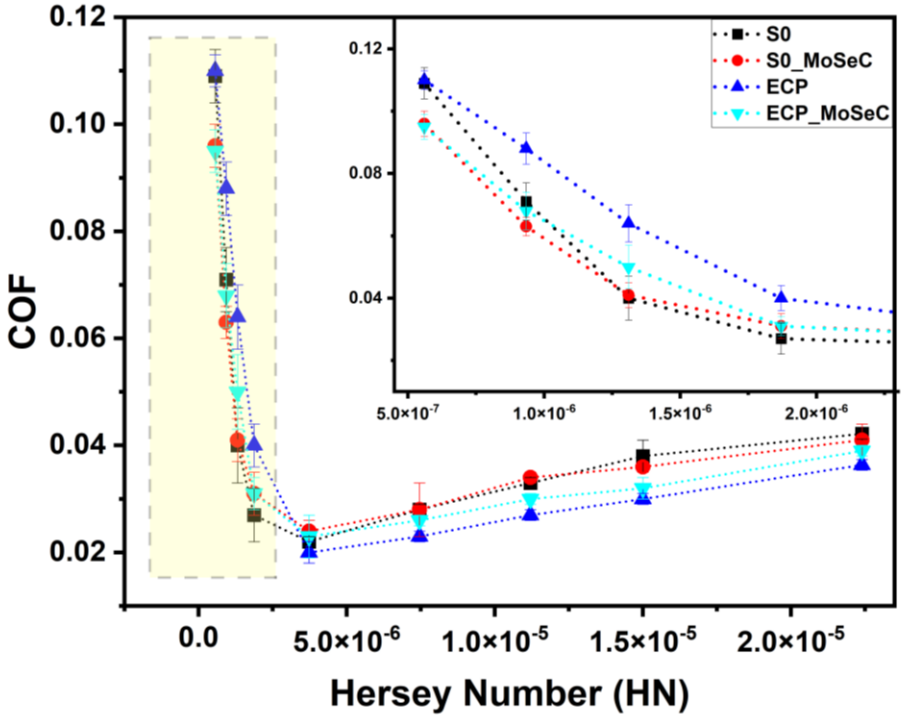

Figure 6. Stribeck curves of S0; S0_MoSeC; ECP_S_C and ECP_S_C_MoSeC.

Table 8. Percentage performance of the S0_MoSeC; ECP_S_C; and ECP_S_C_MoSeC specimens in comparison to S0 (positive values are decreases in friction related to the smooth and uncoated specimen while negative values mean increases in friction).

Speed (m/s)	0.01	0.02	0.03	0.04	0.07	0.16	0.23	0.31	0.47
ECP_S_C_MoSeC	12.8%	4.2%	−25.0%	−14.8%	−4.5%	7.1%	9.1%	15.8%	7.1%
ECP_S_C	−0.9%	−23.9%	−60.0%	−48.1%	9.1%	17.8%	18.2%	21.0%	14.3%
S0_MoSeC	11.9%	10.7%	−2.5%	−14.8%	−9.1%	−1.2%	−1.5%	5.2%	2.3%
S0	-	-	-	-	-	-	-	-	-

From the Stribeck curves shown in Figure 6, it can be observed that the ECP_S_C_MoSeC specimen performed better than the smooth specimen, S0, and better than the smooth and

coated specimen, S0_MoSeC, for rotational speeds between 0.16 and 0.47 m/s under the HL lubrication regime and for 0.01 m/s, under the BL regime. Still, in relation to the uncoated and textured specimen, ECP_Sc only had a lower friction behaviour for speeds between 0.07 and 0.47 m/s where a really synergistic effect existed. This clearly shows that the synergistic effect of surface texturing and surface coating helps in modifying the frictional properties for lubricated applications under controlled conditions.

Similar studies with respect to circular texture patterns using LST techniques were studied, and the improvement in the load-bearing capacities of these dimples at the HL regime was shown. The main reason for this improvement was the capacity to withstand the lubricant at the sliding interface, which reduced COF values in the full-film lubrication regimes [31]. Additionally, the solid lubricant properties of the MoSeC are an interesting characteristic due to the molecular structures of the transition metal atoms. These structures are very strong and are tightly packed with covalent bonding, and their atomic layers are separated by weak van der Waals forces [32]. The strong atomic bonding of the TMD films helps act as a solid lubricant at the sliding interface when there is an asperity and asperity contacts during the BL regime. It can be seen clearly that the improvement in the circular textured-coated ECP_S_C_MoSeC specimen was very promising in boundary lubrication regimes in comparison to ECP_S_C. Thus, the lubrication properties on the steel surface were improved by both surface modification techniques.

3.3.2. Reciprocating Sliding Test

Figure 7 shows the evolution of the COF with the sliding speed for the textured and coated specimen (ECP_S_C_MoSeC) and smooth specimen (S0). It can be seen that the COF was always lower for the textured and coated specimen for the entire range of sliding speeds tested; probably, a synergistic effect of texturing and coating also exists. During the block-on-ring experiment, the contact area between the ring and the disc did not cover enough textures (dimples) required to apprize a true improvement in the textures in all lubricating regimes. To overcome this challenge, the reciprocating sliding experiment with a pin-on-disc configuration was performed. Additionally, as expected, the result observed in Figure 7 shows that there was an overall improvement for the tested low-speed values (Table 9) that confirmed the synergistic effect of the texturing and coating, which was especially evident for the boundary lubrication conditions (lower speed values).

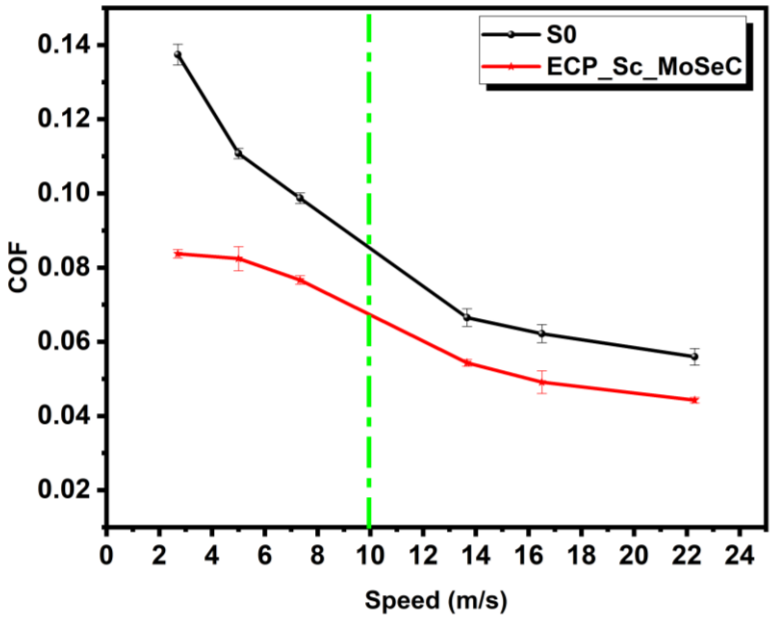

Figure 7. Evolution of the COF with the sliding speed for S0 and ECP_S_C_MoSeC specimens (lubricated with PAO 8).

Table 9. Percentage performance of the ECP_S_C_MoSeC specimen in comparison to S0 (positive values are decreases in friction related to the smooth and uncoated specimen).

Speed (mm/s)	2.7	5	7.3	13.6	16.5	22.3
ECP_S_C_MoSeC	39.1%	25.6%	22.4%	18.4%	21.0%	20.9%
S0	-	-	-	-	-	-

4. Characterization of the Wear Mechanisms from the Textured Specimen (ECP_S_C) and Textured/Coated Specimen (ECP_S_C_MoSeC)

4.1. ECP_S_C Specimen

The textured specimen ECP_S_C surface was analyzed on the SEM after the sliding test. There was no measurable wear on the specimen surface because the number of rotating cycles during the block-on-ring experiment was not sufficient enough to wear the specimen. However, there were traces of minor scratches, as shown in Figure 8B,C. These scratches on the textured surface were observed at the texture boundaries. Additionally, it was observed that these texture boundaries were smooth, and during the sliding interaction helped in supplying the lubricant from the texture storage area. This easy flow resulted in the reduction in COF at ML and HL regimes.

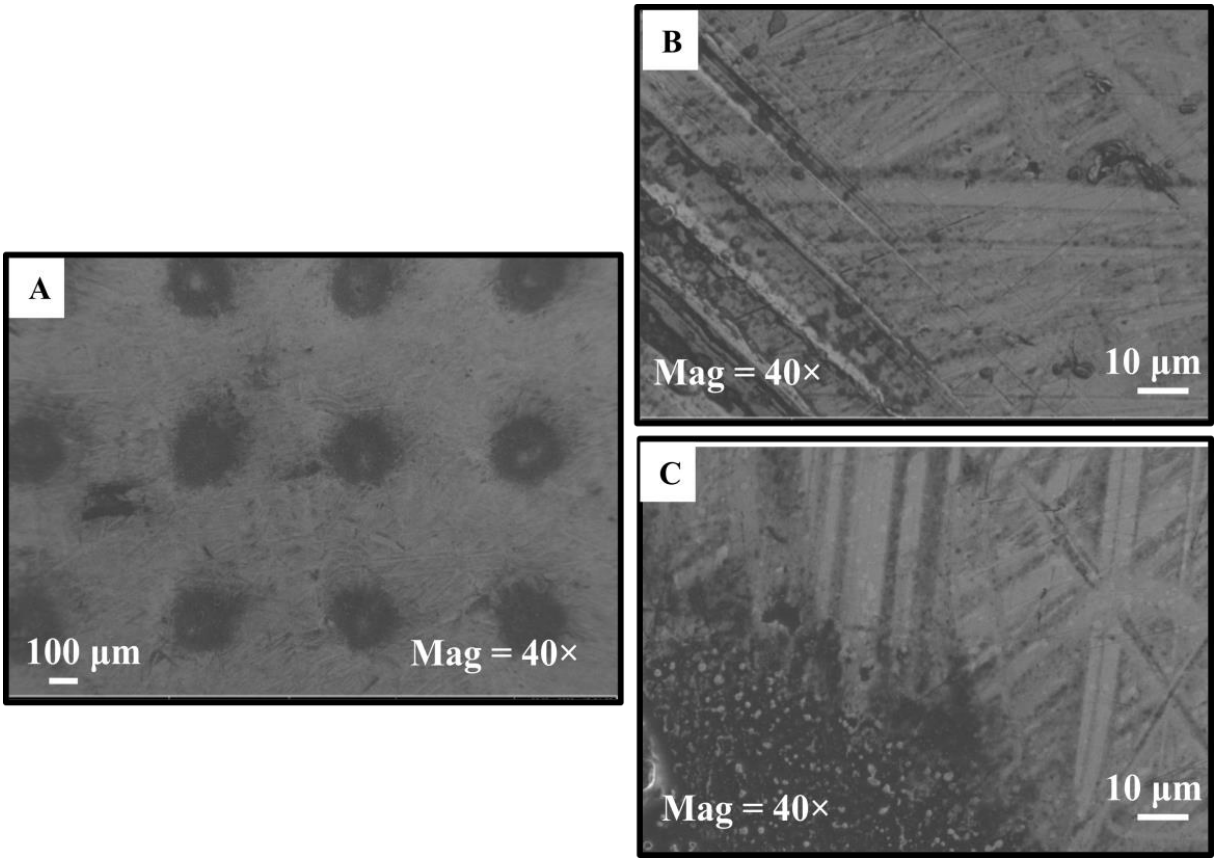

Figure 8. SEM images of ECP_S_C specimen showing: (**A**) Textured surface; (**B**) Scratch on the surface and; (**C**) Scratch at the boundary of the texture.

The ECP textured surfaces (ECP_S_C) were analysed around the texture boundaries via EDS. Figure 9A shows the surface of the ECP_S_C, and (B) represents the magnified region of the texture boundary, whereas Figure 9C depicts the chemical composition of this region.

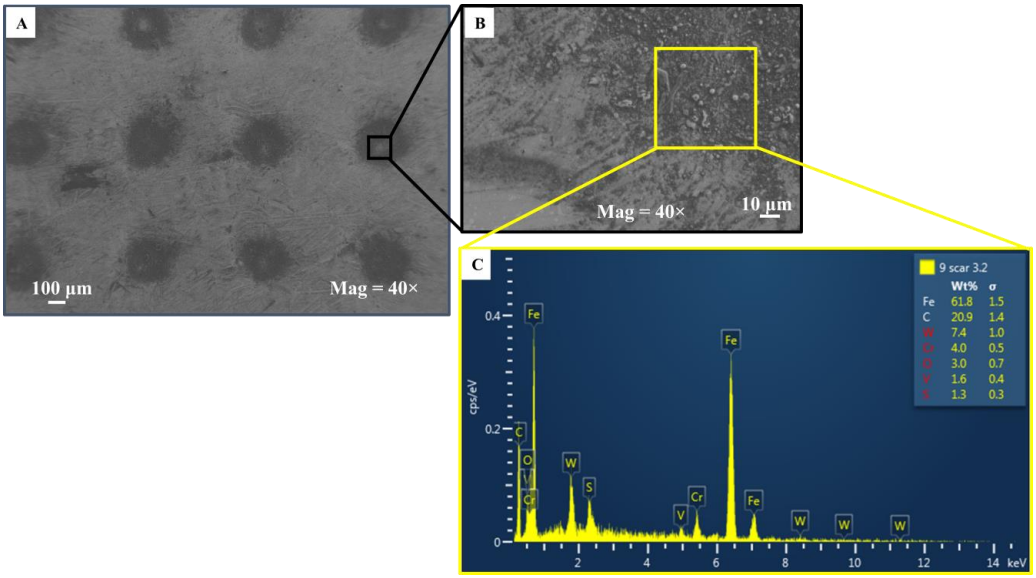

Figure 9. SEM image of ECP_S_C specimen showing: (**A**) Image of textured surface; (**B**) Magnified image of dimple boundary; (**C**) Chemical composition (EDS data) of the magnified area.

4.2. ECP_S_C_MoSeC Specimen

The surface of the textured and coated specimen ECP_S_C_MoSeC was analyzed after the block-on-ring tribometer test. It has been analyzed that there was no presence of any significant wear on the surface. Some traces of the scratches were present, which can be seen in Figure 10A. Furthermore, this scratch was magnified in Figure 10B so that the disintegration of the coating could be seen. In Figure 10B, the marked region shows the complete wear-out region of the coating, which was evident of the solid lubricant nature of the coating and further helped lower down the COF values. This reduction in the friction values in the BL regime was the outcome of these remotions of the coating that acted as the sacrificial layer preventing higher coefficients of friction.

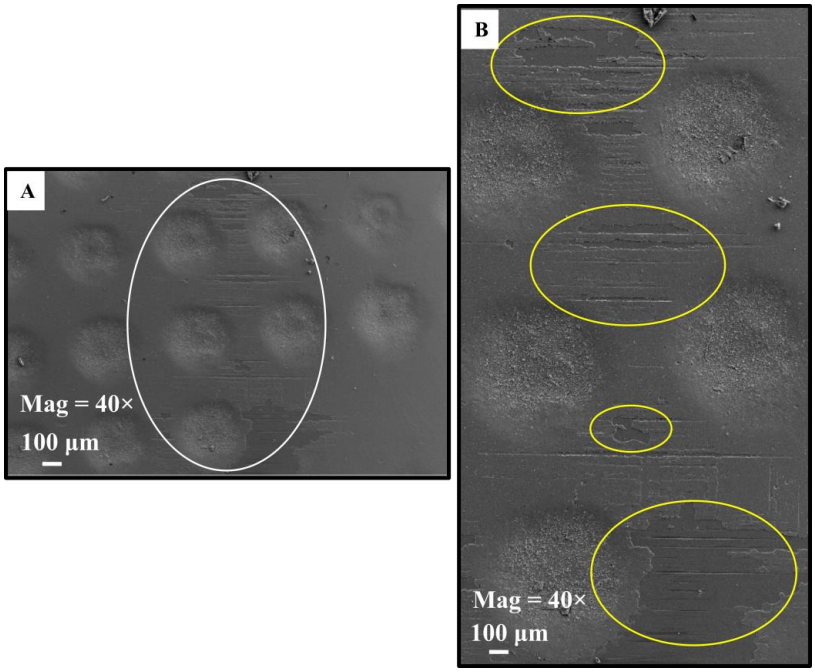

Figure 10. SEM image of the ECP_S_C_MoSeC specimen showing: (**A**) Textured surface; (**B**) Magnified image of the scratches.

The surface of the ECP_S_C_MoSeC specimen was analyzed to check that the traces of the coting contributed to the solid lubrication property of the coating. Figure 11A shows the textured surface of the ECP_S_C_MoSeC and Figure 11B shows the magnified texture area, and Figure 11C shows the EDS data at the magnified surface. It was evident that a similar weight percentage of the metallic composition was present at the surface as in the case of S0_MoSeC. However, the coating provided a significant value of the solid lubricant on the material surface, which contributed to the solid contacts at the BL regime. This significantly helped reduce the coefficient of friction values under BL conditions.

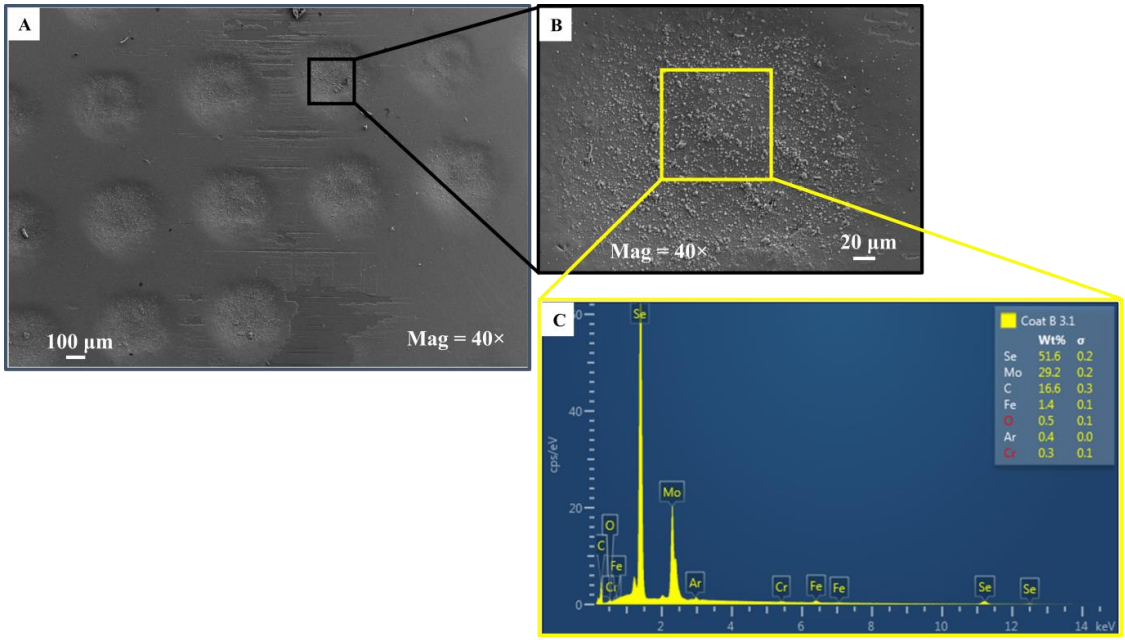

Figure 11. SEM image of ECP_S_C_MoSeC specimen showing: (**A**) Image of textured surface; (**B**) Magnified image of dimple; (**C**) EDS data.

Figures 12 and 13 show the results of the SEM/EDS analysis of the specimens that were, respectively, textured and coated and just coated and submitted to the tribological tests. It can be seen that the coating was removed from the contact zone and only remained inside the textured dimples. It is also possible to observe that part of the Cr interlayer was also removed, exposing the Fe that constituted the substrate. However, it is quite difficult to measure and quantify the wear as the coating was very thin at approximately 1.8 µm thick. Nevertheless, it is possible to see that the lowering of the friction under the boundary lubrication regime was mainly at the expense of the coating, which worked as a sacrificial material.

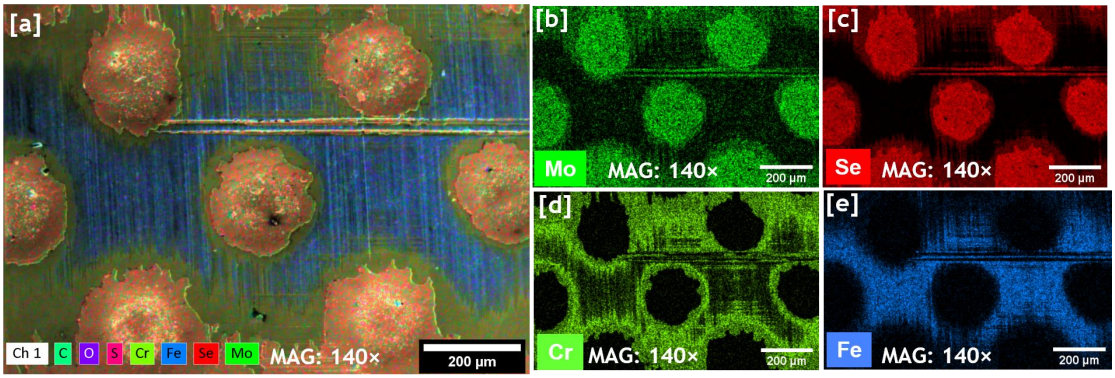

Figure 12. (**a**) SEM/EDS mapping showing the chemical composition distribution for textured and coated specimen ECP_S_C_MoSeC; (**b**) Mo coming from the coating; (**c**) Se coming from the coating; (**d**) Cr from the coating interlayer and (**e**) Fe from the substrate.

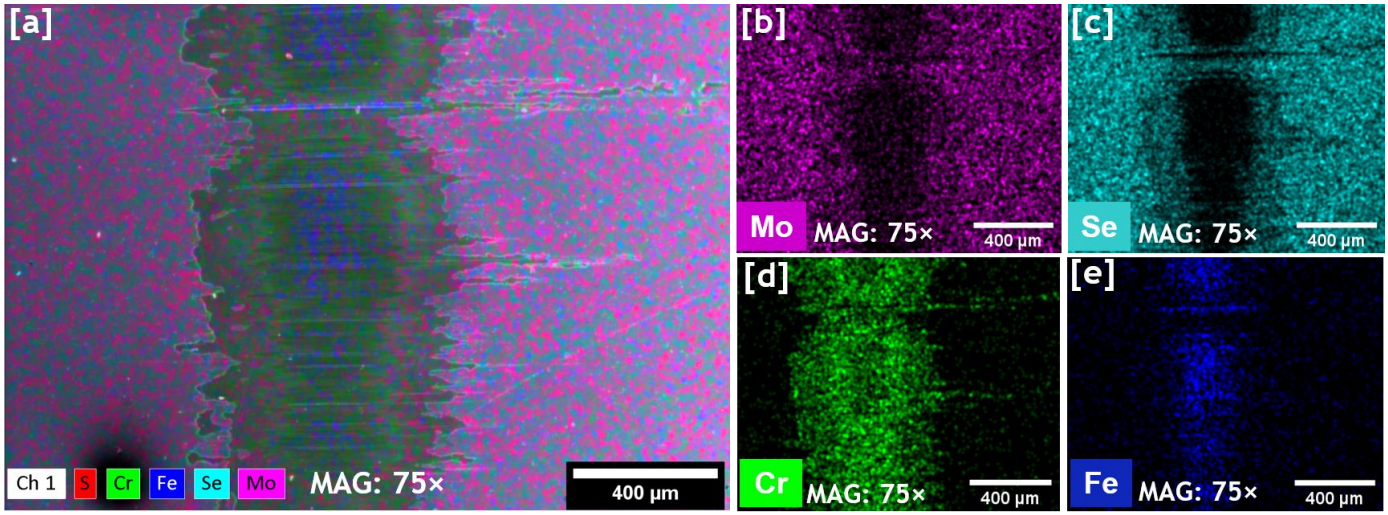

Figure 13. (**a**) SEM/EDS mapping showing the chemical composition distribution for the coated specimen MoSeC; (**b**) Mo coming from the coating; (**c**) Se coming from the coating; (**d**) Cr from the coating interlayer and (**e**) Fe from the substrate.

5. Conclusions

The synergistic study by combining the texturing and coating on the steel specimen has shown that surface coated and textured contributes to improving the frictional properties in the BL regime, where an interaction between the asperities occurred, and the coating worked mainly as a solid lubricant—this benefit is mainly at the expense of the localized destruction of the film, which worked as a sacrificial material. The MoSeC coating improved the tribological properties in relation to the smooth specimen by reducing the COF between 11.9% and 10.7% under the BL regime and between 5.2% and 2.3% under HL conditions. On the other hand, the surface texture played an important role in ML and HL regimes by generating hydrodynamic pressure with a lift-up effect and friction reduction in relation to smooth (S0) and smooth and coated (S0_MoSeC) specimens. In the tribotest trial carried out in which a greater number of dimples were in contact, it proved that the textured and coated specimen always showed a lower coefficient of friction than the smooth specimen.

Author Contributions: Conceptualization, P.S. and A.C.; Data curation, M.R.M. and P.S.; Formal analysis, M.R.M., F.R. and P.S.; Funding acquisition, A.C.; Investigation, M.R.M. and P.S.; Methodology, M.R.M., T.V., L.V. and P.S.; Supervision, A.C.; Validation, A.R. and A.C.; Writing—original draft, M.R.M.; Writing—review and editing, F.R., T.V., L.V., A.R., P.S. and A.C. All authors have read and agreed to the published version of the manuscript.

Funding: This work is sponsored by FEDER and by National funds through FCT-Fundação para a Ciência e a Tecnologia under the projects: ON-SURF ref. "POCI-01-0247-FEDER-024521", ATRITO-0 ref. "POCI-01-0145-FEDER-030446", CEMMPRE ref. "UIDB/00285/2020" and ARISE ref. "LA/P/0112/2020".

Institutional Review Board Statement: Not applicable.

Informed Consent Statement: Not applicable.

Data Availability Statement: The data presented in this study are available on request from the corresponding author. The data are not publicly available due to (the research was performed in the aim of a research project (ATRITO 0)).

Acknowledgments: The authors record sincere thanks to the University of Minho, PMM-Moldes, Instituto Pedro Nunes and CEMMPRE for extending its facilities.

Conflicts of Interest: The authors declare no conflict of interest.

References

1. Bruzzone, A.A.; Costa, H.L.; Lonardo, P.M.; Lucca, D.A. Advances in engineered surfaces for functional performance. *CIRP Ann.* **2008**, *57*, 750–769. [CrossRef]
2. He, D.; Zheng, S.; Pu, J.; Zhang, G.; Hu, L. Improving tribological properties of titanium alloys by combining laser surface texturing and diamond-like carbon film. *Tribol. Int.* **2015**, *82*, 20–27. [CrossRef]
3. Mao, B.; Siddaiah, A.; Liao, Y.; Menezes, P.L. Laser surface texturing and related techniques for enhancing tribological performance of engineering materials: A review. *J. Manuf. Process.* **2020**, *53*, 153–173. [CrossRef]
4. Shum, P.; Zhou, Z.; Li, K. Investigation of the tribological properties of the different textured DLC coatings under reciprocating lubricated conditions. *Tribol. Int.* **2013**, *65*, 259–264. [CrossRef]
5. Meng, R.; Deng, J.; Liu, Y.; Duan, R.; Zhang, G. Improving tribological performance of cemented carbides by combining laser surface texturing and WSC solid lubricant coating. *Int. J. Refract. Met. Hard Mater.* **2018**, *72*, 163–171. [CrossRef]
6. Etsion, I.; Kligerman, Y.; Halperin, G. Analytical and experimental investigation of laser-textured mechanical seal faces. *Tribol. Trans.* **1999**, *42*, 511–516. [CrossRef]
7. Wang, Q.J.; Zhu, D. Virtual texturing: Modeling the performance of lubricated contacts of engineered surfaces. *J. Tribol.* **2005**, *127*, 722–728. [CrossRef]
8. Vilhena, L.; Podgornik, B.; Vižintin, J.; Možina, J. Influence of texturing parameters and contact conditions on tribological behaviour of laser textured surfaces. *Meccanica* **2011**, *46*, 567–575. [CrossRef]
9. Vilhena, L.; Sedlaček, M.; Podgornik, B.; Rek, Z.; Žun, I. CFD modeling of the effect of different surface texturing geometries on the frictional behavior. *Lubricants* **2018**, *6*, 15. [CrossRef]
10. Etsion, I. State of the art in laser surface texturing. *J. Trib.* **2005**, *127*, 248–253. [CrossRef]
11. Ranjan, P.; Hiremath, S.S. Role of textured tool in improving machining performance: A review. *J. Manuf. Process.* **2019**, *43*, 47–73. [CrossRef]
12. Kirchner, V.; Cagnon, L.; Schuster, R.; Ertl, G. Electrochemical machining of stainless-*steel* microelements with ultrashort voltage pulses. *Appl. Phys. Lett.* **2001**, *79*, 1721–1723. [CrossRef]
13. Jain, V. *Micromachining: An Introduction*; Narosa Publishing House: New Delhi, India, 2010; pp. 1.1–1.27.
14. Byun, J.W.; Shin, H.S.; Kwon, M.H.; Kim, B.H.; Chu, C.N. Surface texturing by micro ECM for friction reduction. *Int. J. Precis. Eng. Manuf.* **2010**, *11*, 747–753. [CrossRef]
15. Zeng, Z.; Wang, Y.; Wang, Z.; Shan, D.; He, X. A study of micro-EDM and micro-ECM combined milling for 3D metallic micro-structures. *Precis. Eng.* **2012**, *36*, 500–509. [CrossRef]
16. Chen, X.; Qu, N.; Hou, Z.; Wang, X.; Zhu, D. Friction reduction of chrome-coated surface with micro-dimple arrays generated by electrochemical micromachining. *J. Mater. Eng. Perform.* **2017**, *26*, 667–675. [CrossRef]
17. Yaqub, T.B.; Vuchkov, T.; Evaristo, M.; Cavaleiro, A. DCMS Mo-Se-C solid lubricant coatings–Synthesis, structural, mechanical and tribological property investigation. *Surf. Coat. Technol.* **2019**, *378*, 124992. [CrossRef]
18. Herdan, J. Lubricating oil additives and the environment—An overview. *Lubr. Sci.* **1997**, *9*, 161–172. [CrossRef]
19. Scharf, T.; Prasad, S. Solid lubricants: A review. *J. Mater. Sci.* **2013**, *48*, 511–531. [CrossRef]
20. Fusaro, R.L. Effect of substrate surface finish on the lubrication and failure mechanisms of molybdenum disulfide films. *ASLE Trans.* **1982**, *25*, 141–156. [CrossRef]
21. Polcar, T.; Nossa, A.; Evaristo, M.; Cavaleiro, A. Nanocomposite Coatings of Carbon-Based and Transition Metal Dichalcogenides Phases: A Review. *Adv. Mater. Sci* **2007**, *15*, 118–126.
22. Brainard, W.A. *The Thermal Stability and Friction of the Disulfides, Diselenides, and Ditellurides of Molybdenum and Tungsten in Vacuum (109 to 106 Torr)*; National Aeronautics and Space Administration: Washington, DC, USA, 1968.
23. Vitu, T.; Huminiuc, T.; Doll, G.; Bousser, E.; Matthews, A.; Polcar, T. Tribological properties of Mo-SC coating deposited by pulsed dc magnetron sputtering. *Wear* **2021**, *480*, 203939. [CrossRef]
24. Wang, G.; Zhao, G.; Song, J.; Ding, Q. Study on tribological properties of TMDs-coated copper from the nanoscale. *Mater. Today Commun.* **2022**, *31*, 103815. [CrossRef]
25. Kubart, T.; Polcar, T.; Kopecký, L.; Novák, R.; Nováková, D. Temperature dependence of tribological properties of MoS2 and MoSe2 coatings. *Surf. Coat. Technol.* **2005**, *193*, 230–233. [CrossRef]
26. Polcar, T.; Evaristo, M.; Cavaleiro, A. Comparative study of the tribological behavior of self-lubricating W–S–C and Mo–Se–C sputtered coatings. *Wear* **2009**, *266*, 388–392. [CrossRef]
27. Vilhena, L.; Ramalho, A.; Cavaleiro, A. Grooved surface texturing by electrical discharge machining (EDM) under different lubrication regimes. *Lubr. Sci.* **2017**, *29*, 493–501. [CrossRef]
28. Veltkamp, B.; Velikov, K.; Venner, C.; Bonn, D. Lubricated friction and the Hersey number. *Phys. Rev. Lett.* **2021**, *126*, 044301. [CrossRef] [PubMed]
29. Tallian, T. Rolling bearing life modifying factors for film thickness, surface roughness, and friction. *J. Lubr. Technol.* **1981**, *103*, 509–516. [CrossRef]
30. Caessa, J.; Vuchkov, T.; Yaqub, T.B.; Cavaleiro, A. On the microstructural, mechanical and tribological properties of Mo-Se-C coatings and their potential for friction reduction against rubber. *Materials* **2021**, *14*, 1336. [CrossRef]

31. Amoroso, P.J.; Ramalho, A.; Richhariya, V.; Silva, F.S.; Cavaleiro, A. Tribological performance of laser-textured steel surfaces in unidirectional sliding line-contact (block-on-ring). *Lubr. Sci.* **2021**, *33*, 417–431. [CrossRef]
32. Hudec, T.; Izai, V.; Satrapinskyy, L.; Huminiuc, T.; Roch, T.; Gregor, M.; Grančič, B.; Mikula, M.; Polcar, T. Structure, mechanical and tribological properties of MoSe2 and Mo-Se-N solid lubricant coatings. *Surf. Coat. Technol.* **2021**, *405*, 126536. [CrossRef]